

1 **Discharge-driven rapid bank-erosion and its impact on sediment budgeting in lower**
2 **Ganga valley: Evidences from Malda district, West Bengal, India**

3 Saptarshi Dey¹, Abhirup Basu², Sudeep N. Banerjee³, and Vikrant Jain³

4 1 – Discipline of Earth Sciences, IIT Gandhinagar, Palaj-382055, Gujarat, India.

5 2 – Department of Geology, Presidency University, Kolkata-700073, West Bengal, India.

6 3 – Indian Institute of Technology Gandhinagar, Palaj-382055, Gujarat, India.

7

8 [This work is under review in EPISODES with the article reference number #
9 EPISODES-D-21-00076. This manuscript therefore is a non-peer reviewed preprint
10 submitted to EarthArXiv. The manuscript doi will be updated once the manuscript is
11 accepted for publication]

12

13 **Discharge-driven rapid bank-erosion and its impact on sediment budgeting in lower**
14 **Ganga valley: Evidences from Malda district, West Bengal, India**

15 Saptarshi Dey¹, Abhirup Basu², Sudeep N. Banerjee³, and Vikrant Jain³

16 1 – Discipline of Earth Sciences, IIT Gandhinagar, Palaj-382055, Gujarat, India.

17 2 – Department of Geology, Presidency University, Kolkata-700073, West Bengal, India.

18 3 – Indian Institute of Technology Gandhinagar, Palaj-382055, Gujarat, India.

19 **Abstract**

20 Riverbank erosion coupled with recurrent flooding has been a persistent problem in
21 large parts of the Eastern India. Published data on bank erosion of the Ganga River in West
22 Bengal suggests an annual average of 8 sq. km. land-loss during 1969-1999 and that
23 potentially affected lives of nearly a million people and destroyed various human
24 establishments. In this study, we aim to constrain the spatiotemporal change in the path of the
25 Ganga River and its impact of on sediment reworking in the plains area. For this, we used
26 LANDSAT imagery from the year 1987 to 2019. Our analysis is based on a MATLAB-based
27 toolbox called RivMAP. We show that the mean reach-averaged migration rates of the Ganga
28 River vary from 200-600m/yr. Over the last three decades, the Malda district suffered a land-
29 loss of ~140 km², yielding an average annual loss of 4.5 km². First order mass estimate
30 suggests ~30 Mt/yr sediment yield from the Ganga riverbank in Malda, which is ~8–15% of
31 the total annual sediment load of the large Ganga River expected in Farakka Barrage. In the
32 end, this study highlights the role of climate on river migration and bank erosion.

33 **Keywords**

34 Ganga; Riverbank erosion; river migration; sediment flux; discharge.

35 **1. Introduction**

36 The Ganga River is one of the most important river of the Indian subcontinent as for
37 not only the human dependency on it, but also for its' geopolitical aspects (Nearly forty
38 million people depend directly or indirectly on the Ganga River and the Ganga River basin is
39 one of the fertile sectors for agriculture). The Ganga River is one of the largest sediment
40 dispersal systems characterized by high sediment load. Extensive siltation in the main Ganga
41 River channel and its tributaries is responsible for reduction in channel capacity and frequent
42 flooding, especially in the eastern Ganga plains (Jain and Sinha, 2003, Sinha et al., 2005).
43 Further, downstream reaches of the Ganga River channel, especially the lower Ganga valley
44 (Fig. 1a) has also been dominated by bank erosion process leading to channel migration.
45 Frequent changes in the Ganga River-path have made headlines in international media over
46 the last few decades. Unfortunately, though some notable studies have been done on Ganga
47 migration by Philip et al., (1989), Jain and Ahmed (1993), Shukla et al., (2012), Thakur et al.,
48 (2012) and Mukherjee and Pal (2018) – there exists very limited knowledge on the
49 quantitative aspects of bank erosion, river migration at annual time scale and its implication
50 on reach-scale sediment budgeting.

51 Remote sensing-based analysis provides an excellent tool to study the spatio-temporal
52 variability in bank erosion processes (e.g., Thakur et al., 2012; Hassan, 2015; Payne et al.,
53 2018). Nanson and Hickin (2012) measured later-migration rate and volume of eroded
54 sediment in various meandering rivers of western Canada. Their studies highlighted
55 significant relationship between bank erosion and sediment transport characteristics. Further,
56 time-series remote sensing data have been used with probabilistic approach to assess channel
57 instability and to predict bank-erosion prone area in near future (Graf, 1984; 2000). Recent
58 advancements in remote sensing studies provides an important tool to achieve improved
59 understanding of spatio-temporal variability in bank erosion processes of the Ganga River.

60 Extensive bank erosion along alluvial reaches may also govern the sediment load in
61 the channel. A conceptual model provided by Hooke (2003) highlights that contribution from
62 bar and bed erosion may act as an important sediment source for coarse sediment in a river
63 channel. A recent study from a suburban Chesapeake Bay watershed, USA having 1.5×10^5
64 km^2 watershed shows dominance (>90%) of bank-derived material in river sediment
65 (Cashman et al., 2018). However, this important process has mostly been ignored in sediment
66 budgeting of the Ganga River and its tributaries. A regional scale suspended-load based
67 sediment budgeting of the Ganga-Brahmaputra River basin suggested almost 100% sediment
68 from the Himalayan region, and insignificant sediment contribution from the plains (<10%)
69 and peninsular India (<10%) (Wasson, 2003). Though, significant sediment contribution
70 through bank erosion has been observed in smaller Himalayan rivers namely Burhi Gandak
71 and Kamla Balan River (Sinha and Friend, 1994; Sinha and Jain, 1998), such understanding
72 and quantitative data on sediment fluxes from bank erosion are lacking from the main Ganga
73 River channel. Limitation of sediment flux data to understand the connectivity structure of
74 the Ganga Plains has been highlighted in a conceptual study on geomorphic connectivity
75 (Jain and Tandon, 2010).

76 In this study, we explored the upper part of the lower Ganga valley. We selected ~100
77 km traverse upstream from the geopolitically important Farakka barrage. Geographically it
78 falls in the district of Malda, West Bengal (cf. Fig.1 for location and geographic extent). We
79 quantified the planform changes in the river-path by analyzing multispectral remote sensing
80 imagery of the last three decades, to be specific from 1987 to 2019. With this study, we
81 highlight the annual-to-decadal scale changes in channel migration rate and compute areas of
82 land accretion/ land loss due to river migration. Our work underlines the significance of bank
83 erosion in alluvial plains in the total sediment budget of a large river. This work on the 100

84 km long stretch of the Ganga River indicates the total sediment contribution from alluvial
85 plains may be significant in the total sediment budgeting of a river system.

86 **2. Description of the study area**

87 The Ganga River originates from the Gangotri glacier in the western Himalaya and
88 flows ~2900 km till it meets the Bay of Bengal (Fig. 1a). The Ganga River and its tributaries
89 originating from the western and the central Nepal Himalaya are major source of water in the
90 Indo-Gangetic Plains. More importantly, the Ganga drainage basin delivers a massive amount
91 of sediment each year to the submarine depo-centers (e.g., Lupker et al., 2011; Wasson,
92 2003). Over centennial to millennial scales, the sediment budget can be as high as 610 ± 230
93 Mt/yr (Lupker et al., 2012). Over annual-decadal scale, several studies have come up with a
94 range of estimates. There exist a few older studies from Bangladesh which portray a range of
95 200–550 Mt/yr (Coleman, 1969; BWDB). Average sediment budget measured for Ganga
96 River in Bangladesh is ~ 390 Mt/yr (Lupker et al., 2011 and references therein). In Farakka,
97 India (our study area), Abbas and Subramanian (1984) estimated the annual sediment load to
98 be ~ 728 Mt. Recently, a study by Khan et al., (2018) report average annual sediment load at
99 Farakka to be ~200 Mt (data from CWC, Govt. of India). On the other hand, the discharge
100 measured far from the Himalaya, is dependent mostly on monsoonal rainfall. Monthly
101 discharge at the Indo-Gangetic plain is highly biased towards the monsoonal month (Khan et
102 al., 2018; Singh et al., 2007; Rao, 1975). Monthly hydrographs show that nearly 80% of the
103 annual discharge is related to the monsoonal months (July-October) (Rao, 1975). Measured
104 15-year average annual discharge at Farakka is $3807 \times 10^3 \text{ m}^3/\text{s}$ (Khan et al., 2018; CWC data
105 from 1994-2008) (<http://www.cwc.gov.in>).

106 Our study area is situated in the upstream part of the lower Ganga valley (Fig. 1a).
107 The lower Ganga valley starts from the eastern end of Bihar, easterly to the confluence of

108 Kosi with Ganga River (cf. Fig.1a). The Ganga River takes a southerly turn near the town of
109 Sahibganj and it enters the state of West Bengal and flows southwards till the Farakka
110 barrage (Fig. 1b). The western flank of the Ganga River in this 100-110 km stretch is covered
111 mostly by the Rajmahal hills and its' characteristic basalts. Riverbank erosion is the biggest
112 problem in the districts of Malda on either side of the Farakka barrage. Riverbank migration
113 and flooding in this area is a recurring headline during monsoon months in national and
114 international news media. Sinha and Ghosh (2011) favor that the oscillation and
115 geomorphological changes in the Ganga River in this stretch is due to the existence of the
116 Farakka barrage. According to reports by several official surveys, ~8 km² area is wiped out
117 annually by erosion of the Ganga Riverbank in West Bengal (Das et al., 2014). During 1979-
118 1999, approx. 3850 Hectares (~40 km²) of land was lost due to bank erosion in Malda
119 (Rudra, 2000). The land loss data show a rise during 1995-1999. Therefore, estimation of the
120 following decades is crucial. It is estimated that nearly half a million people were affected by
121 recurrent flood in the Ganga River in this stretch over the past couple of decades.

122 **3. Materials and methods**

123 Our work is based on remotely-sensed satellite images from LANDSAT data
124 repository spanning from 1987 to 2019 ([https://www.usgs.gov/core-science-](https://www.usgs.gov/core-science-systems/nli/landsat)
125 [systems/nli/landsat](https://www.usgs.gov/core-science-systems/nli/landsat)). We used the data from the month of December of every year as it
126 contains the least cloud-cover. Clear images of the years 1998, 2002, 2007 and 2012 were not
127 found and therefore ignored for the analysis. From 1987 to 2011, LANDSAT-5 has been used
128 whereas; from 2013 LANDSAT-8 images are available. Then for images of all the 29 years,
129 the Near Infrared (NIR), Short-wave infrared-1 (SWIR-1) and red bands were used for
130 producing false color composite. The composite image was classified into 6 classes using the
131 “Iso Cluster Unsupervised Classification” tool in ArcGIS. With this classification the water
132 pixels became distinctly identifiable. The classified image was again reclassified by giving

133 the water pixels a value of 1 and all the other pixels a value of 0. This reclassified raster was
134 converted into a polygon by and the polygon was edited to separate out the ‘hydrologically-
135 connected’ segment of the river by setting the values of all the other features as 0. Similarly,
136 the single threaded component was also separated out. Finally, these hydrologically
137 connected and single threaded components were again converted back into raster files. In this
138 manner, the binary channel masks (both hydrologically connected and single threaded
139 component) were prepared for all the 29 years. For the analysis, we have used the ‘single-
140 threaded component’ in this study. We acknowledge that this involves ignoring several
141 narrow channels associated with the main channel during computation. But the cumulative
142 area for those narrow channels is $< 5 - 8\%$ of the main channel. So, that can be counted as a
143 methodological uncertainty. These binary Channel Masks were then converted into ‘.mat’
144 format and the .mat file was run in MATLAB R2019a environment. We primarily followed
145 the codes provided by the RivMap toolbox (Schwenk et al., 2016). The modified code used in
146 this study is given in Appendix A. Figure 3 illustrates the key methodology adopted for this
147 study.

148 **4. Results**

149 The processed LANDSAT images from different years point out drastic changes in
150 the channel pattern, channel width and most importantly the spatial shift in drainage (Fig. 4).
151 To avoid complexity in calculation, we used the mainstem river for our analysis of total bank
152 erosion, annual reach-averaged river migration and erosional/ accretional areas. The
153 mainstem river selection is mentioned as ‘St’ method in RivMAP (Schwenk et al., 2017).

154 **4.1. Migration mapping and channel migration rate**

155 Fig. 5 illustrates how the channel has migrated within the time period of 1987-2019. It
156 illustrates that the lateral migration or meandering of the mainstem river is most prominent in

157 the upper part of the study area (up to the town of Rajmahal) where two distinct loops of
158 meanders are visible. Fig. 5 tells us that the meanders grew over the last three decades. The
159 extent of migration is ~8–10 km in the meandering zone. Channel migration in the lower part
160 of the study area is low and shows more or less channelized flow of the mainstem river, the
161 width or the migration is also minimal. However, during 2006-2012, channel widening is
162 seen in the southern part. The total erosion/ accretion area is plotted in Supplementary Fig.
163 S1.

164 Computed average migration rates vary from 200 to 600 m/yr (Fig. 6). This is the
165 riverbank migration rate. Centerline migration rates are provided in Supplementary Fig. S2.
166 Migration rates are high (>400 m/yr) during 1998-2002 (except 2001), 2009-2013 (except
167 2010) and 2016.

168 **4.2. Riverbank erosion/ accretion rate and cumulative area analysis**

169 Annual bank erosion rates vary from 5 to 22 km during 1987–2019. This represents
170 the average length of riverbank eroded per year. The accretion rate eventually lower and in
171 the range of 2–7 km/yr. Therefore, in this time window, erosion dominates over accretion and
172 we face land loss. Surface area calculation for eroded and accreted area was done using the
173 difference between two consecutive years. Pixel values are multiplied by each pixel area (900
174 m²). Fig. 7b illustrates land erosion/ accretion through time. In 32 years, the total erosion was
175 ~255 km² while accretion was only ~105 km². Erosion was faster during 1995–1998,
176 2000–2002 and 2009-2013. The slope of the cumulative accretion hints nearly uniform
177 accretion through time. The net land loss is ~140 km² (Fig. 7c)

178 **4.3. Land loss**

179 During 1987-2001, the net land loss was increasing steadily and the average channel
180 width was also increasing (Fig. 7c). This was the major phase of channel widening. Looking
181 at the migration map (Fig. 6), we see that channel widening as well as meandering has
182 happened in the northern part of the study area up to the town of Rajmahal. The meandering
183 loop increased with time, increasing the channel sinuosity. During 2001-2005, the channel
184 width was steady and so was the net land loss. During this time, accretion was at par with
185 erosion, so net land loss was minimal. Then, during 2006-2012, the channel width was
186 reduced although the rate of land loss picked up (Fig. 7b). This can be explained by change in
187 the river pattern. Prior to 2006, the mainstem river was wide. But somewhere in between
188 2003 and 2008, possibly around 2006, the channel pattern changed to anabranching, as
189 number of anabranches across floodplains have been observed (cf. Fig. 4). Therefore, the
190 width of the mainstem river declined, but its' numerous branches started to erode. Since
191 2012, the rate of land loss as well as the mainstem channel width declined. The anabranching
192 of the river reduced while the mainstem river got wider and since then, the mainstem river is
193 contributing to the bank erosion.

194 **5. Discussion**

195 LANDSAT image analysis using RivMAP toolbox in MATLAB (Schwenk et al.,
196 2016) has enabled us to detect and quantify planform changes in river pattern of a part of the
197 Lower Ganga valley. In the following text, we discuss how we used the outputs to quantify
198 erosion over annual-decadal scale. We also discuss the reason behind rapid erosion of the
199 riverbank and implications of our study.

200 **5.1. Channel migration and river dynamics**

201 Over the last three decades or even over the last half a century, the trajectory of the
202 Ganga River in Malda district has changed (Thakur et al., 2012). But the change is not

203 uniform or steady throughout its' course. Moreover, different parts of the traverse have
204 different planform geometry. Interestingly, in the years when migration rates are high (1998-
205 2002, 2009-2013 and 2016) (Fig. 6), the annual discharge is also high (CWC data; Pal and
206 Pani, 2016) and the flood hazard is also high (DFO Flood observatory)
207 (<http://floodobservatory.colorado.edu/SiteDisplays/51.htm> (Accessed 10 June 2021)).

208 Migration map in Fig. 5 suggest that the upper part of the study area is affected
209 strongly by meandering. We see two large meander loops which grow opposite to each other
210 with time (cf. Fig. 5 where white arrows mark the spatiotemporal shift). Loop 1, near
211 Sahibganj, has grown ~8 km towards SSW; whereas, loop 2, in between Sahibganj and
212 Rajmahal has grown ~4.5 km towards NNE. With this trend, the town of Sahibganj in Bihar,
213 will be under threat in few years' time. The town of Rajmahal is fairly safe. The southern part
214 of the trajectory has very small evidences of meandering and rather follow a direct N-S path
215 till Farakka. The migration map of this area does not show big lateral shifts. But we must
216 mention that this part of the trajectory is characterized by anabranching of the river channel
217 (cf. Fig. 4, time slice 2008, 2011). The reason for changing the channel pattern may be linked
218 to change in slope. But with existing field/ DEM data, it is very hard to verify.

219 **5.2. Control of discharge on erosion**

220 As the monsoon arrives in Bengal, recurrent events of bank erosion get the attention
221 of the media. Thus, we favor to test the role of rainfall on bank erosion. Monsoon brings
222 more water in the channel; therefore, river discharge data and surface runoff data are
223 important. River discharge data and runoff data of the station Rajmahal (station id: 51) for the
224 duration of 1999–2019 were downloaded from the DFO Flood Observatory
225 (<https://floodobservatory.colorado.edu/>). The data is based on microwave radiometry
226 (Brakenridge et al., 2021). The rainfall distribution in Indian Sub-continent is heavily non-

227 uniform and positively biased for the monsoon months (June-September) (Rao, 1975). In
228 Rajmahal station, the discharge and runoff are high in end-monsoon to post-monsoon months
229 of August to November (Supplementary Fig. S3). Thus, we used the peak discharge data for
230 correlation (possibly September- October). To test the correlation of peak discharge and
231 runoff with our new erosion rates, we fit linear regression using 95% confidence interval
232 (Fig. 8). Regression fit for the discharge (Fig. 8a) is much better ($R^2 = 0.83$) than the same for
233 runoff (Fig. 8b) ($R^2 = 0.26$). This clearly hint that peak discharge is the key driving factor for
234 river-bank erosion. That underlines the fact that the stronger monsoon in the upstream or
235 even sudden influx of flooding in the channel would warrant destruction of the river-bank.
236 The local rainfall is probably not that significant, else, we would have seen a better
237 correlation with surface runoff (Fig. 8b). Similar high correlation is seen when we compare
238 migration rate with peak discharge ($R^2 = 0.80$) (Fig. 8c) than with runoff ($R^2 = 0.23$) (Fig.
239 8d). Therefore, we may conclude that migration rate and erosion rate co-vary with each other
240 and both are controlled by discharge (a proxy of climate).

241 **5.3. Implication of bank erosion on sediment budgeting**

242 Fig. 7a shows annual variations in erosion and accretion in the study area. More often,
243 erosion is higher than accretion. The scenario is further elaborated in Fig. 7b which portray
244 annual change in cumulative erosion and accretion within the study area. As erosion is much
245 stronger than accretion within the reach, therefore, the study area records a net land loss in
246 the stipulated time-period (Fig. 7c). Especially, during 1996-2002 and 2009-2012, the erosion
247 was high. In Fig. 7c, we portray the net land loss (area) with time. $\sim 140 \text{ km}^2$ land has been
248 eroded along reach of $\approx 100 \text{ km}$ in last 30–32 years, which results in an annual average of 4.4
249 km^2/yr . Considering the average bank height to be $\sim 3\text{m}$ (Fig. 2 – field photos) and bulk
250 density of cohesive soil to be 2000–2200 kg/m^3 , a rough estimate of annual eroded mass will

251 be ~26 - 29 Mt from \approx 100 km length of the study reach. Or in other words, the sediment
252 yield is 0.26 – 0.29 Mt per km length of the channel per year. Considering the annual average
253 sediment load at downstream station at Farakka or at Harding Bridge, Bangladesh as
254 200–390 Mt (Lupker et al., 2011; Khan et al., 2018), we claim that 8–15% of the sediment
255 load is derived from erosion of the river-bank from 100 km stretch within the Malda district,
256 West Bengal. Considering the total length of the river in the alluvial plains as \sim 1800 km, the
257 contribution from the plains area could be much higher. This finding highlights the role of
258 significance of alluvial area as a sediment source at modern time scale within the Gangetic
259 foreland basin.

260

261 **6. Conclusion**

262 By combining the results from LANDSAT image analysis and comparing them with
263 remotely-sensed flow parameters from the study area, we conclude the following –

- 264 1. The Ganga River in the Malda district of West Bengal is causing land loss due to
265 channel migration. The northern part of the district is facing problems due to increase
266 in meandering while the southern part is facing an eastward shift of the channel.
- 267 2. High correlation between annual bank erosion rate and annual peak discharge for the
268 duration of 1999–2018 underlines the dominant control of climate on river-bank
269 erosion.
- 270 3. The total land loss along \approx 100 km long reach over the last 3 decade is \sim 140 km²,
271 yielding an erosion rate of 4.4 km²/yr. Considering an average bank height of \sim 3m,
272 the annual sediment yield from this part of the Ganga River is \sim 26–29 Mt.

273 **Acknowledgement**

274 S. Dey is supported by DST-INSPIRE Faculty Fellowship grant
275 (#DST/INSPIRE/04/2017/003278). We thank Chaitali Biswas and Tanmoy Bhaduri for the
276 field photographs and information used in this work.

277 **References**

278 Abbas, N. and Subramanian, V., 1984. Erosion and sediment transport in the Ganges river
279 basin (India). *Journal of Hydrology*, 69 (1–4), 173–182. doi:10.1016/0022-1694(84) 90162-8.

280 Biswas, R., & Anwaruzzaman, A. K. M. (2019). Measuring hazard vulnerability by bank
281 erosion of the Ganga river in Malda district using PAR model. *Journal of Geography,*
282 *Environment and Earth Science International*, 22(1), 1-15.

283 Brakenridge, G. R., Kettner, A. J., Paris, S., Cohen, S., Nghiem, S. V. River and Reservoir
284 Watch Version 4.0. DFO Flood Observatory, University of Colorado, USA.
285 <http://floodobservatory.colorado.edu/SiteDisplays/51.htm> (Accessed 12 June, 2021).

286 Coleman, J.M., 1969. Brahmaputra River: channel processes and sedimentation. *Sedimentary*
287 *Geology*, 3 (2–3), 129– 239. doi:10.1016/0037-0738(69)90010-4.

288 Das, B., Mondal, M., & Das, A. (2012). Monitoring of bank line erosion of River Ganga,
289 Malda District, and West Bengal: Using RS and GIS compiled with statistical techniques. *Int*
290 *J Geomat Geosci*, 3(1), 239-248.

291 Das, T.K., Haldar, S.K., Dasgupta, I., and Sen, S., "River Bank Erosion Induced Human
292 Displacement and Its Consequences", *Living Rev. Landscape Res.*, 8 (2014), 3.

293 Goodbred, S.L., Kuehl, S.A., 1999. Holocene and modern sediment budgets for the Ganges–
294 Brahmaputra river system: evidence for highstand dispersal to flood-plain, shelf and deep-sea
295 depocenters. *Geology* 27, 559–562.

296 Graf, W. L. (1984). A probabilistic approach to the spatial assessment of river channel
297 instability. *Water Resources Research*, 20(7), 953-962.

298 Graf, W. L. (2000). Locational probability for a dammed, urbanizing stream: Salt River,
299 Arizona, USA. *Environmental Management*, 25(3), 321-335.

300 Hassan, M. S. (2015). Quantification of River Bank erosion and bar deposition in Chowhali
301 Upazila, Sirajganj District of Bangladesh: a remote sensing study. *Journal of Geoscience and*
302 *Environment Protection*, 4(1), 50-57.

303 Hooke, J. (2003). Coarse sediment connectivity in river channel systems: a conceptual
304 framework and methodology. *Geomorphology*, 56(1-2), 79-94.

305 Jain, S. K., & Ahmad, T. (1993). Migration behaviour of river ganga between Allahabad and
306 Buxar using remotely sensed data. *Journal of the Indian Society of Remote Sensing*, 21(1),
307 37-43.

308 Jain, V. and Sinha, R. (2003) River systems in the Gangetic plains and their comparison with
309 the Siwaliks: A review. *Current Science*, 84(8), 1025-1033.

310 Jain, V. and Tandon, S.K. (2010) Conceptual assessment of (dis)connectivity and its
311 application to the Ganga river dispersal system. *Geomorphology*, 118, 349-358.

312 Khan, S., Sinha, R., Whitehead P., Sarkar S., Jin L., & Futter, M.N. (2018) Flows and
313 sediment dynamics in the Ganga River under present and future climate scenarios,
314 *Hydrological Sciences Journal*, 63:5, 763-782, DOI: 10.1080/02626667.2018.1447113.

315 Lupker, M., Blard, P. H., Lavé, J., France-Lanord, C., Leanni, L., Puchol, N., Charreau, J., &
316 Bournès, D. (2012). 10Be-derived Himalayan denudation rates and sediment budgets in the
317 Ganga basin. *Earth and Planetary Science Letters*, 333, 146-156.

318 Lupker, M., France-Lanord, C., Galy, V., Lave', J., Gaillardet, J., Gajurel, A., Guilmette, C.,
319 Rahman, M., Singh, S., Sinha, R., 2012. Predominant floodplain over mountain weathering of

320 Himalayan sediments (Ganga basin). *Geochim. Cosmochim. Acta* 84, 410–432,
321 <http://dx.doi.org/10.1016/j.gca.2012.02.001>.

322 Lupker, M., France-Lanord, C., Lave', J., Bouchez, J., Galy, V., Me'tivier, F., Gaillardet, J.,
323 Lartiges, B., Mugnier, J.L., 2011. A Rouse-based method to integrate the chemical
324 composition of river sediments: application to the Ganga basin. *JGR—Earth Surface* 116,
325 F04012, <http://dx.doi.org/10.1029/2010JF001947>.

326 [Matthew J. Cashman](#), [Allen Gellis](#),[Lillian Gorman Sanisaca](#),[Gregory B. Noe](#),[Vanessa](#)
327 [Cogliandro](#),[Anna Baker](#). 2018. Bank-derived material dominates fluvial sediment in a
328 suburban Chesapeake Bay watershed. *River Research and Applications*,
329 <https://doi.org/10.1002/rra.3325>

330 Mukherjee, K., & Pal, S. (2018). Channel migration zone mapping of the River Ganga in the
331 Diara surrounding region of Eastern India. *Environment, Development and*
332 *Sustainability*, 20(5), 2181-2203.

333 Nanson, G. C., & Hickin, E. J. (1986). A statistical analysis of bank erosion and channel
334 migration in western Canada. *Geological Society of America Bulletin*, 97(4), 497-504.

335 Pal, R., Pani, P. Seasonality, barrage (Farakka) regulated hydrology and flood scenarios of
336 the Ganga River: a study based on MNDWI and simple Gumbel model. *Model. Earth Syst.*
337 *Environ.* 2, 57 (2016). <https://doi.org/10.1007/s40808-016-0114-x>

338 Payne, C., Panda, S., & Prakash, A. (2018). Remote sensing of river erosion on the Colville
339 River, North Slope Alaska. *Remote Sensing*, 10(3), 397.

340 Philip, G., Gupta, R. P., & Bhattacharya, A. (1989). Channel migration studies in the middle
341 Ganga basin, India, using remote sensing data. *International Journal of remote*
342 *sensing*, 10(6), 1141-1149.

343 Rao, K.L., 1975. India's Water Wealth. Oxford University Press, London. 475 pp.

344 Rudra, K. (2000). Living on the edge: the experience along the bank of the Ganga in Malda
345 district, West Bengal. *Indian Journal of Geography & Environment*, 5, 57-67.

346 Schwenk, J., Khandelwal, A., Fratkin, M., Kumar, V., & Fofoula-Georgiou, E. (2017). High
347 spatiotemporal resolution of river planform dynamics from Landsat: The RivMAP toolbox
348 and results from the Ucayali River. *Earth and Space Science*, 4(2), 46-75.

349 Shukla, U. K., Srivastava, P., & Singh, I. B. (2012). Migration of the Ganga River and
350 development of cliffs in the Varanasi region, India during the late Quaternary: Role of active
351 tectonics. *Geomorphology*, 171, 101-113.

352 Singh, I.B., Bajpai, V.N., Kumar, A., Singh, M., 1990. Changes in the channel characteristics
353 of Ganga River during Late Pleistocene– Holocene. *Journal of the Geological Society of*
354 *India* 36, 67–73.

355 Singh, M., Singh, I. B., & Müller, G. (2007). Sediment characteristics and transportation
356 dynamics of the Ganga River. *Geomorphology*, 86(1-2), 144-175.

357 Sinha, R, Jain, V., Prasad Babu, G. and Ghosh, S. (2005) Geomorphic characterization and
358 diversity of the rivers of the Gangetic plains. *Geomorphology*, 70, 207-225.

359 Sinha, R. and Ghosh, S., 2012. Understanding dynamics of large rivers aided by satellite
360 remote sensing: a case study from Lower Ganga plains, India. *Geocarto International*, 27 (3),
361 207–219. doi:10.1080/10106049.2011.620180.

362 Sinha, R. and Jain, V. (1998) Flood hazards of north Bihar rivers, Indo-Gangetic Plains. In:
363 Kale, V.S. (ed.) *Flood studies in India*; Geological Society of India, Memoir 41, 27-52.

364 Sinha, R. and Jain, V. (1998) Flood hazards of north Bihar rivers, Indo-Gangetic Plains. In:
365 Kale, V.S. (ed.) *Flood studies in India*; Geological Society of India, Memoir 41, 27-52.

366 Sinha, R., & Friend, P. F. (1994). River systems and their sediment flux, Indo-Gangetic
367 plains, Northern Bihar, India. *Sedimentology*, 41(4), 825-845.

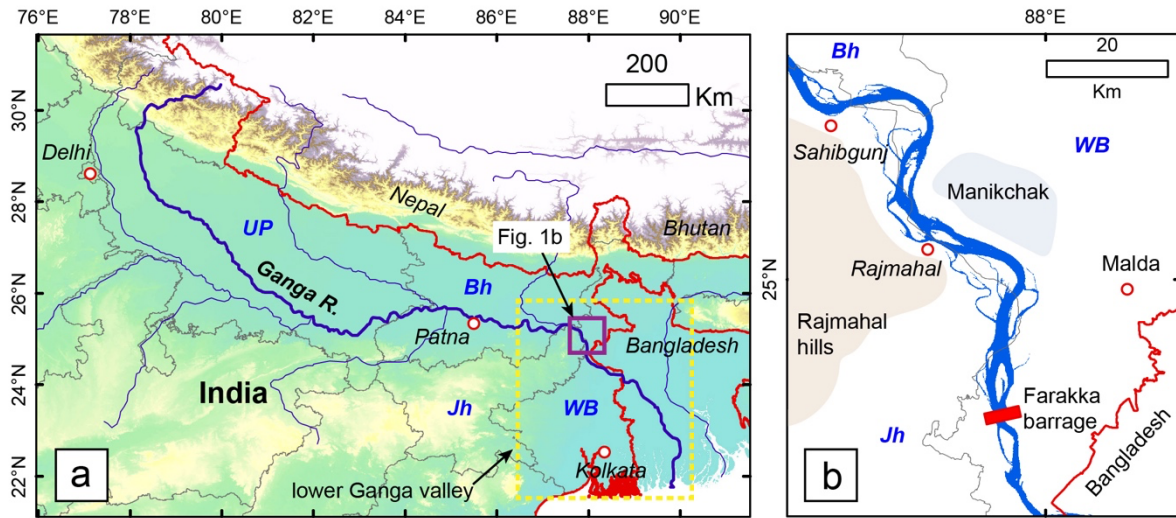
368 Sinha, R., & Friend, P. F. (1994). River systems and their sediment flux, Indo-Gangetic
369 plains, Northern Bihar, India. *Sedimentology*, 41(4), 825-845.

370 Srivastava, P., Sharma, M., Singhvi, A.K., 2003. Luminescence chronology of incision and
371 channel pattern changes in the Ganga River, India. *Geomorphology* 51, 259–268.

372 Thakur, P. K., Laha, C., & Aggarwal, S. P. (2012). River bank erosion hazard study of river
373 Ganga, upstream of Farakka barrage using remote sensing and GIS. *Natural Hazards*, 61(3),
374 967-987.

375 Wasson, R. J. (2003). A sediment budget for the Ganga–Brahmaputra catchment. *Current*
376 *science*, 1041-1047.

377 **Figures**



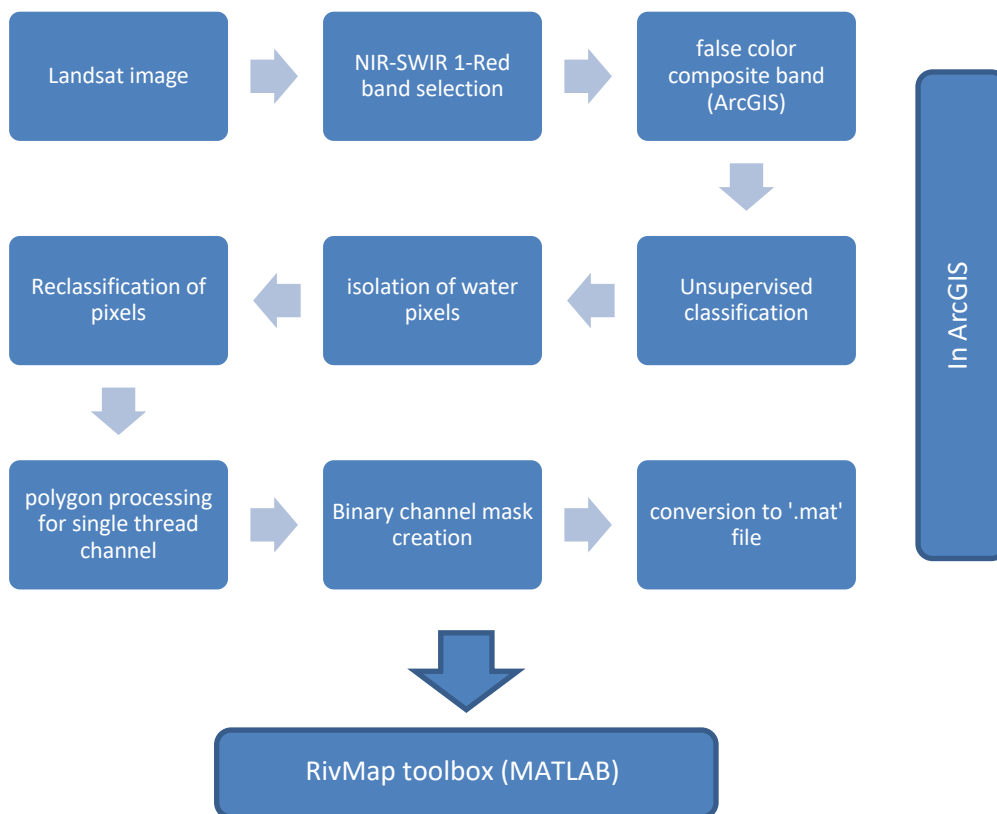
378

379 Figure 1: (a) An overview map of the Ganga basin showing the geographic boundaries
380 (labelled in blue font) and our study area as purple rectangle. (b) Enlarged view of the study
381 area showing the present-day track of the Ganga River (as in December, 2019) and the
382 important towns/ places along the river. The lower bound of our study area is the Farakka
383 barrage. [Abbreviations: UP – Uttar Pradesh, Bh – Bihar, WB- West Bengal, Jh –
384 Jharkhand].



385

386 Fig. 2: Field photographs. (a) human establishments at eroding bank of the Ganga River near
 387 Manikchak, Malda. (b) Eroding Ganga riverbank at Samsorganj, Murshidabad (downstream
 388 from Farakka Barrage). (c) Migration of Ganga River engulfing the cultivation land in Malda.
 389 (d) Villages in Kaliachak, Malda are facing the threat of abolishment due to river migration.



390

391

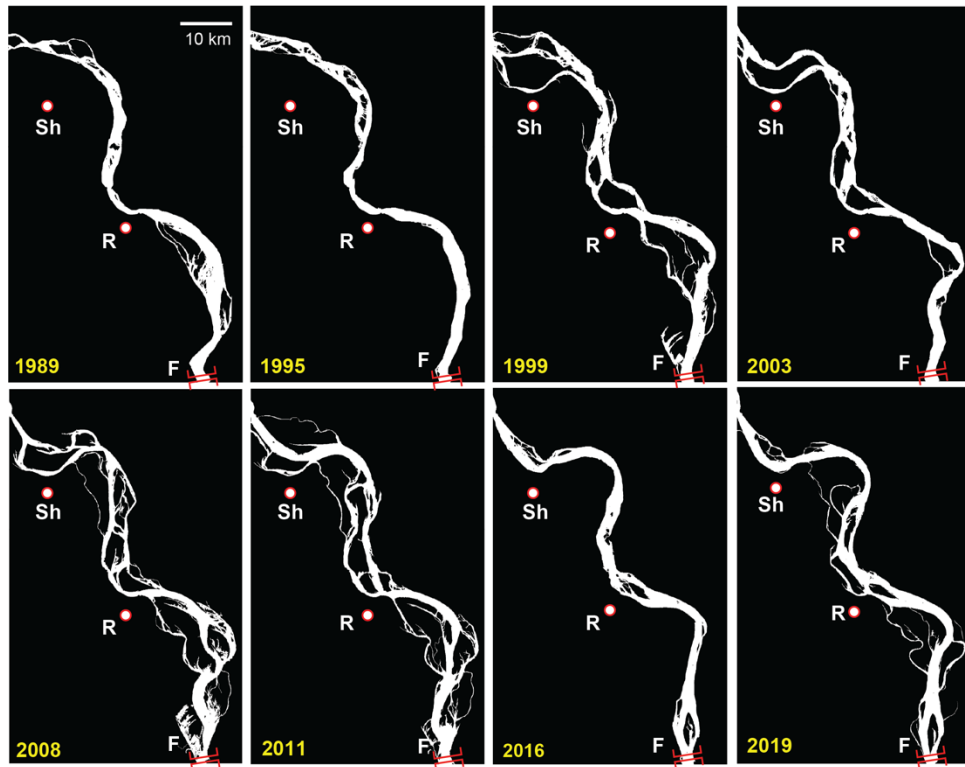
392

393

394

395 Fig. 3: A conceptual flowchart explaining the methodological steps adopted for this study.

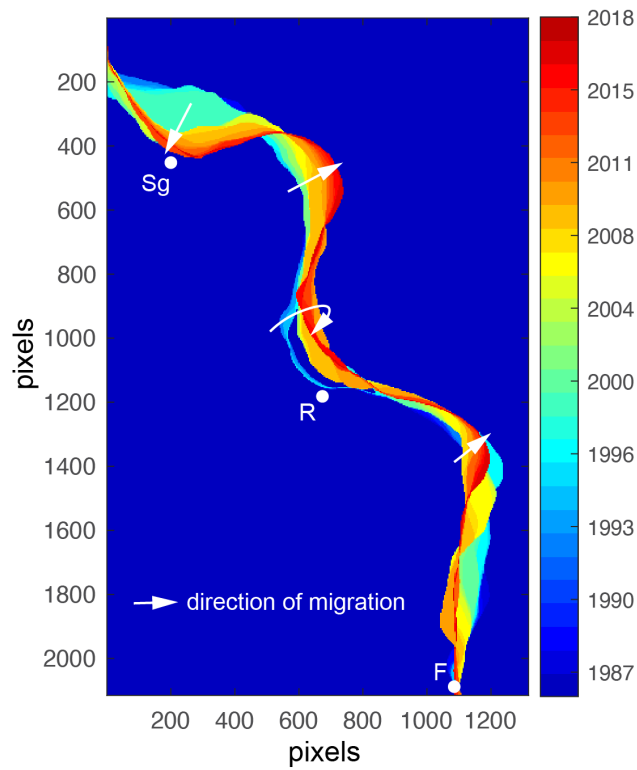
396 This process has been repeated for 29 datasets spanning from 1987 till 2019.



397

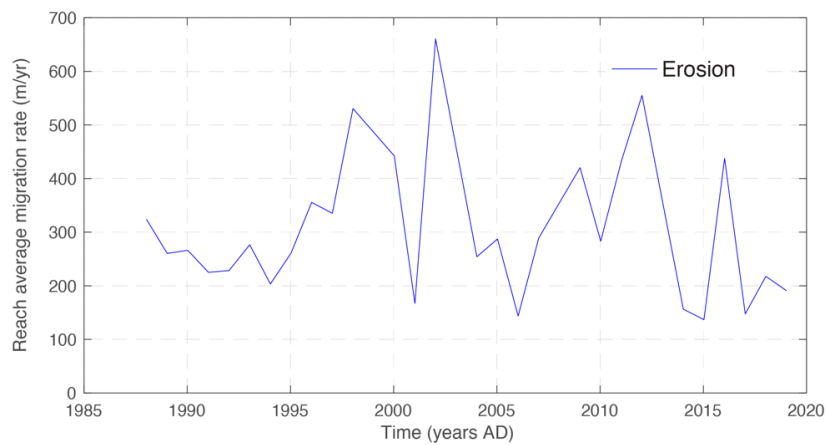
398 Fig. 4: Classified LANDSAT images from different years (mentioned in yellow text) show
399 changes in drainage pattern and spatial shift in drainage over the last 3 decades.

400 [Abbreviations: Sh- Sahibganj, R- Rajmahal, F- Farakka].



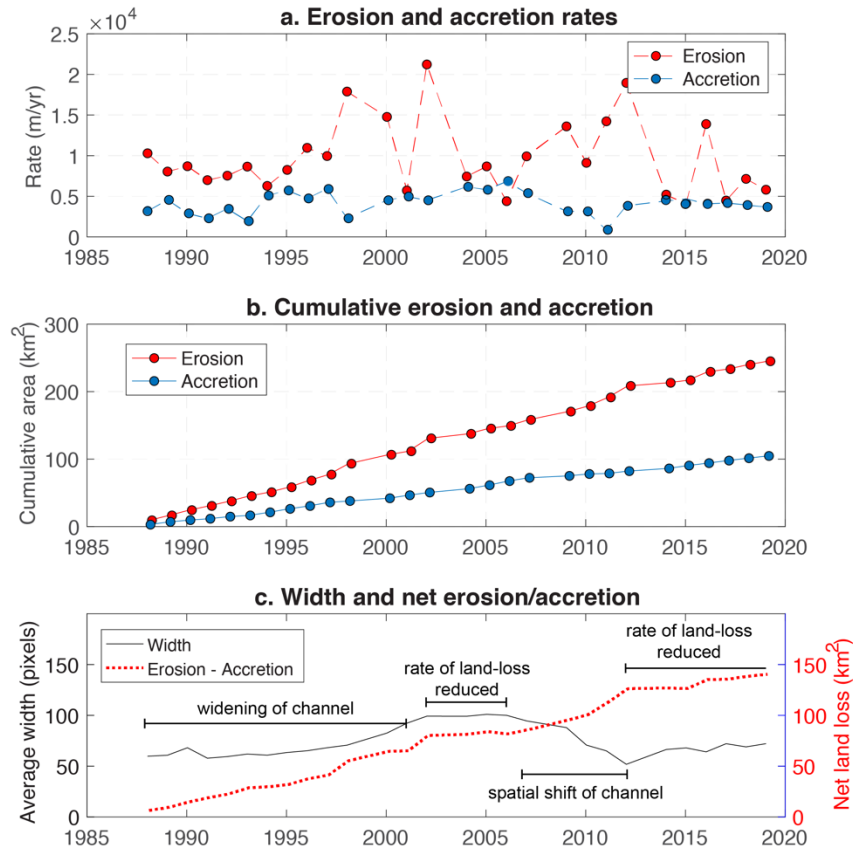
401

402 Fig. 5: Channel migration map of the study area showing annual shift in channel path and
 403 overall increase in meander in the upper part of the study area. Temporal migration of the
 404 channel is indicated by arrows.



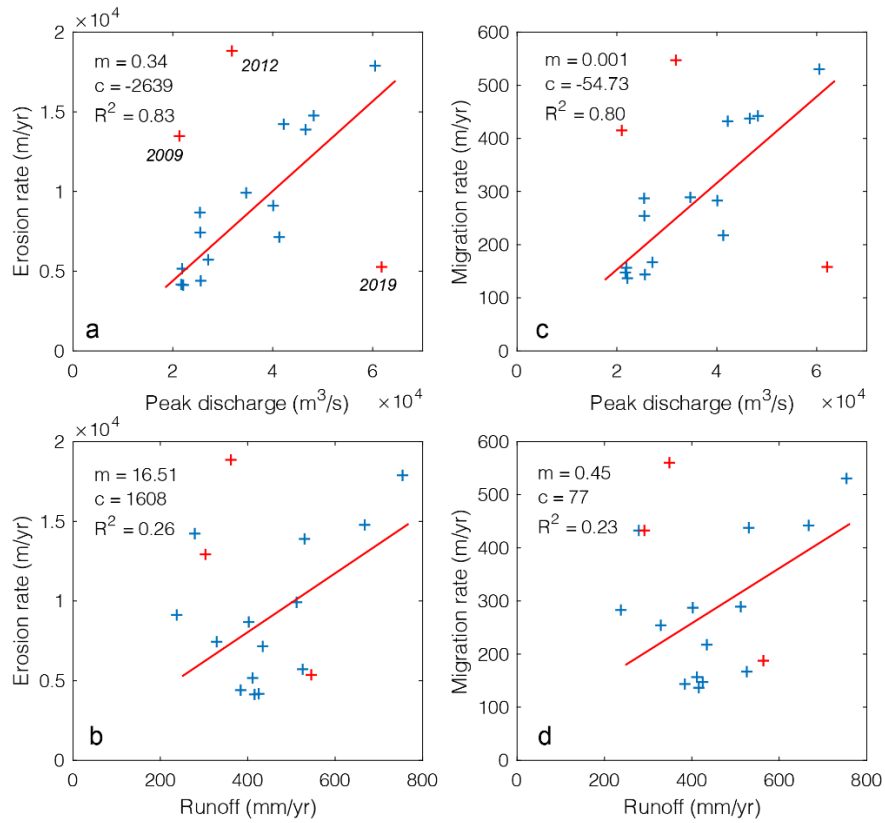
405

406 Fig. 6: Reach-averaged migration rate over the last 3 decades. CL stands for centerline
 407 migration while Erosion indicates bank migration. Both the trends are identical and major
 408 migration happened in 1997, 2000 and 2010.



409

410 Fig. 7: (a) Annual bank erosion rate vs. accretion rate throughout the study area. This portrays
 411 how much km of riverbank has been eroded/ accreted per year. (b) Cumulative area of
 412 erosion and accretion are plotted against time. It shows that erosion is faster than accretion,
 413 therefore, the study area is facing land-loss. (c) Net loss is predicted from the difference
 414 between cumulative erosion and accretion. The slope of the blue line tells that over the last
 415 decade land-loss slowed down than 2000-2010. The average channel width also decreased
 416 since 2010.



417

418 Fig. 8: Scatter-plot exploring relationship of erosion rate with (a) peak annual discharge and
 419 (b) annual runoff for the duration of 1999-2018. Microwave radiometry-based discharge and
 420 runoff data are collected from DFO flood observatory
 421 (<https://floodobservatory.colorado.edu/>). Linear fit parameters are obtained by using 95%
 422 confidence interval. Peak discharge shows a better fit ($R^2 = 0.83$) than runoff ($R^2 = 0.26$). We
 423 ignored data from 2003, 2009 and 2012 (marked in red) while calculating regression-fit as we
 424 consider them as outliers. Similar results are obtained using migration rate with peak
 425 discharge (Fig. 8c) and runoff (Fig. 8d).